Published in final edited form as:

FASEB J. 2022 April ; 36(4): e22254. doi:10.1096/fj.202101873RR.

ArhGEF12 activates Rap1A and not RhoA in human dermal microvascular endothelial cells to reduce tumor necrosis factor-induced leak

Alamzeb Khan[1], **Weiming Ni**[1], **Tania Baltazar**[2], **F. Lopez-Giraldez**[3], **Jordan S. Pober**[2], **Richard W. Pierce**[1]

[1]Department of Pediatrics, Yale School of Medicine, Yale University

[2]Department of Immunobiology, Yale School of Medicine, Yale University

[3]Department of Genetics, Yale School of Medicine, Yale University

Abstract

Overwhelming inflammation in the setting of acute critical illness induces capillary leak resulting in hypovolemia, edema, tissue dysoxia, organ failure and even death. The tight junction (TJ)-dependent capillary barrier is regulated by small GTPases, but the specific regulatory molecules most active in this vascular segment under such circumstances are not well described. We set out to identify GTPase regulatory molecules specific to endothelial cells (EC) that form TJs. Transcriptional profiling of confluent monolayers of TJ-forming human dermal microvascular ECs (HDMECs) and adherens junction only forming-human umbilical vein EC (HUVECs) demonstrate *ARHGEF12* is basally expressed at higher levels and is only downregulated in HDMECs by junction-disrupting tumor necrosis factor (TNF). HDMECs depleted of ArhGEF12 by siRNA demonstrate a significantly exacerbated TNF-induced decrease in trans-endothelial electrical resistance and disruption of TJ continuous staining. ArhGEF12 is established as a RhoA-GEF in HUVECs and its knock down would be expected to reduce RhoA activity and barrier disruption. Pulldown of active GEFs from HDMECs depleted of ArhGEF12 and treated with TNF show decreased GTP-bound Rap1A after four hours but increased GTP-bound RhoA after 12 hours. In cell-free assays, ArhGEF12 immunoprecipitated from HDMECs is able to activate both Rap1A and RhoA, but not act on Rap2A-C, RhoB-C or even Rap1B which shares 95% sequence identity with Rap1A. We conclude that in TJ-forming HDMECs, ArhGEF12 selectively activates Rap1A to limit capillary barrier disruption in a mechanism independent of cAMP-mediated Epac1 activation.

Corresponding author: Richard W. Pierce, Richard.pierce@yale.edu, Pediatric Critical Care Medicine, 333 Cedar Street, PO Box 208064, New Haven, CT, 06520.

AUTHOR CONTRIBUTIONS

RWP conceived and funded the research, RWP and JSP reviewed all results and provided feedback for all experiments, interpretation, and analysis. AK and WN performed the research experiments and analyzed data. TB performed experiments and provided assistance in data analysis. FLG performed all bioinformatic analysis. AK, RWP and JSP wrote the manuscript, all authors participated in manuscript revision and approved the final draft.

This work was conducted at Yale University in the Vascular Biology and Therapeutics Program

Conflict of interest statement: No authors have any conflicts of interest to disclose.

DISCLOSURES

No authors have any relevant disclosures.

Subject codes:

Inflammation; permeability; Rho Guanine Nucleotide-exchange factor; GTPase signaling; trans-endothelial electrical resistance; electrical cell substrate impedance sensing; capillary leak; vascular dysfunction

INTRODUCTION

Endothelial cell (EC) monolayers line the lumen of continuous capillaries and create a permselective barrier between blood and tissues(1). These ECs actively maintain this barrier by forming intercellular tight junctions (TJs), characterized by claudin-5 and zona-occludins-1 (ZO1)(2). In the setting of localized inflammation, post-capillary venular ECs, which lack TJs found in capillaries, phosphorylate and internalize adherens junction (AJs) proteins to retract cell borders to allow physiologic paracellular leak(3). This flux of fluid and cells produces two of the cardinal signs of inflammation; *tumor* and *dolor*, but results in minimal systemic symptoms(4). Because capillary barrier integrity is contingent on TJs, it is normally preserved in the setting of localized inflammation. Persistent or overwhelming systemic inflammation however, as seen in clinical entities such as sepsis or after cardiac arrest, induces breakdown of TJ-dependent capillary barriers allowing unregulated flux of fluid and cells across the microcirculatory networks, a clinical phenomenon called capillary leak(5). Due to its massive cumulative surface area, leak across capillary segments is pathologic and results in distributive shock, tissue swelling and dysoxia, multi-organ failure and even death(6). There are no treatments for capillary leak, due in large part to our lack of understanding of the complex regulation of capillary TJ disassembly and recovery. A better understanding of how the TJ-dependent capillary barrier is regulated may provide new insights and treatments for human diseases.

The capillary barrier, and the organization of the TJ molecules that form it, is regulated in large part by the activity of GTPases. GTPases are a family of hydrolase enzymes that function as molecular switches and cycle between an active, GTP-bound conformation and an inactive, GDP-bound conformation. GTPase activity state cycling is controlled by guanine nucleotide exchange factors (GEFs) and GTPase-activating proteins (GAPs). GEFs catalyze the exchange of GDP for GTP, thereby activating effector GTPases whereas GAPs accelerate the intrinsically slow GTP hydrolysis of GTPases, leading to functional inactivation(7, 8). When active with bound GTP, different GTPases activate effector kinases that ultimately act to promote or diminish EC junctional integrity. The best studied of these are in the RhoGTPase family and include Rac1 and Cdc42, both of which are essential to form and maintain EC barriers(9), as well as RhoA and RhoB, which act to disrupt the vascular barrier(10). RhoA has been primarily characterized in human umbilical vein ECs (HUVECs) while RhoB is a potent negative regulator of capillary permeability(11, 12).

Other GTPases in the Ras superfamily, namely Ras-related proteins (Raps), also regulate EC barrier function. Humans express five Rap proteins: Rap1A and -B and Rap2A, -B and -C which share roughly 60% sequence identity(13, 14). Rap1 consists of two very similar proteins, Rap1A and Rap1B(14), which share 95% sequence identity. Generally, Rap1 and −2 family members act antagonistically, with active Rap1 proteins promoting

and Rap2 proteins destabilizing the EC barrier(15). Rap1A null mice have altered myeloid cell function and are generally viable(16), whereas vascular-targeted dual removal of Rap1A and -B is lethal by E10.5 suggesting overlapping effects essential for vasculature development(17). In human umbilical vein ECs (HUVECs), Rap1A plays a significant role in AJ stability(18) while Rap1B exacerbates vascular endothelial growth factor induced leak(19), suggesting unique functions. Identification of the primary or partial contributions of specific isoforms to capillary barrier function is significant as these pathways may be uniquely targeted pharmacologically(20). Rap1A and -B have several known GEFs, including the cyclic adenosine monophosphate regulated EPAC (*RAPGEF3*), a well-studied pathway in HUVECs(21).

The regulatory GAPs, GEFs and GTPases that regulate the capillary EC barrier and TJs have not been clearly defined, a significant knowledge gap in our understanding of capillary leak. Importantly, the majority of investigations of Rap functions have been carried out in HUVECs which do not form TJs under standard culture conditions(2). In this study, we utilize cultured human dermal microvascular endothelial cells (HDMECs) because monolayers of these cells form morphological and functional TJs and therefore can serve as an in vitro model of continuous capillaries(2). We report that *ARHGEF12* is differentially expressed in HDMECs compared to HUVECs under basal conditions and after stimulation tumor necrosis factor (TNF). We demonstrate that ArhGEF12 serves to limit disruption of barrier function and tight junction organization in HDMECs after TNF stimulation and that it does so through highly specific activation of Rap1A but not RhoA. Finally, using cell-free assays, we detail the unique specificity of ArhGEF12 for Rap1A and RhoA but not Rap1B, which cannot be explained by structure alone. These findings shed new light on GAP, GEF and GTPase regulation of the capillary barrier.

MATERIALS AND METHODS

Isolation culture of human dermal microvascular endothelial cells

Cultures of human dermal microvascular ECs (HDMECs), isolated from de-identified and discarded normal adult human skin provided through tissue collection service of the Yale University Department of Pathology, and serially passaged as previously described.[21] The Yale University Institutional Review Board has classified this as not human subject research. Serially passaged cultured HDMECs express both the lymphatic EC markers Prox-1 and podoplanin but also uniformly respond to TNF by expressing blood vascular EC markers E-selectin and VCAM-1, which are not expressed by lymphatic ECs in situ(22) suggesting a phenotypic transformation in culture to novel phenotype displaying a mixture of lymphatic, postcapillary, capillary and venous EC properties. Critical for the present study, cultured HDMECs spontaneously and uniformly express TJ molecules claudin 5 and zona occludins 1 (ZO1) and localize these to cell junctions, forming morphologically detectable TJs by confocal immunofluorescence (IF) microscopy and transmission electron microscopy (TEM). These junctions are functional, allowing HDMEC monolayers cultured in commercially available and standardized microvascular media (EGM2-MV, Lonza) to spontaneously form high resistance barriers to electric current assessed by ECIS that resist disruption by calcium chelation(2).

Human umbilical vein endothelial cells (HUVECs) were purchased from Yale University Vascular Biology and Therapeutics Program (https://medicine.yale.edu/vbt/order/) and are uniformly CD31 positive and CD45 negative, form calcium chelation-sensitive VE-cadherin-positive AJs at confluence and uniformly express E-selectin in response to TNF. Although HUVECs express ZO1 and claudin-5 at confluence and these molecules may localize to the cell periphery(23, 24), their distribution does not result in the morphological appearance of TJs by confocal IF or TEM and HUVECs do not form functional TJs across monolayers, i.e. their maximal resistance to electric current is substantially lower than that of HDMECs and they remain susceptible to disruption by calcium chelation even when cultured in EGM2-MV(2). HUVECs may be induced to form TJ under specific culture conditions, such as with compounds to increase cAMP-Epac1-Rap1 activity(25, 26), oxidized phospholipids(27) or co-culture with astrocytes or astrocyte conditioned media(28). Our strategy is to exploit the differences between HDMEC and HUVEC confluent monolayers under EGM2-MV standard culture conditions to identify processes associated with spontaneous formation and TNF-mediated disruption of functional TJs.

Analysis of mRNA expression levels

HDMECs and HUVECs were serially cultured in EGM2-MV and used at passage levels 3 to 6 at 2 to 3 days post-confluence in a 12 well plate (Falcon) and stimulated with 1 ng/mL TNF (Invitrogen) for 6 hours. Cell monolayers were washed with sterile phosphate buffered saline (PBS, Invitrogen) and total RNA was purified using the RNAeasy Mini Kit (Qiagen) with an on-column DNase treatment. For purified total RNA collected from HDMECs samples, strand-specific sequencing libraries were produced following the Illumina TruSeq stranded protocol. According to Illumina protocol, the libraries underwent 76-bp paired-end sequencing using an Illumina HiSeq 2500, generating an average of 32 million paired-end reads per library. For each read, the first 6 and the last nucleotides were trimmed to the point where the Phred score of an examined base fell below 20 using in-house scripts. If, after trimming, the read was shorter than 45 bp, the whole read was discarded. Trimmed reads were mapped to the human reference genome (hg38) with HISAT2 v2.1.0(29) indicating that reads correspond to the reverse complement of the transcripts. Alignments with quality score below 20 were excluded from further analysis. Gene counts were produced with StringTie v1.3.3b(30) and the Python script “prepDE.py” provided in the package. StringTie was limited to reads matching the reference annotation GENCODE v27(31). After obtaining the matrix of read counts, differential expression analysis was conducted, and normalized counts were produced using DESeq2(32). p-values were adjusted for multiple testing using the Benjamini-Hochberg procedure(33). Sequencing data for the HDMECs have been previously deposited in NCBI’s Gene Expression Omnibus (GSE161021). New HUVEC sequencing results for this study are deposited in under accession number GSE190181.

Trans-endothelial electrical resistance measurements

Trans-endothelial electrical resistance (TEER) of HDMEC monolayers was assessed by electrical cell-substrate impedance sensing (ECIS; Applied Biophysics)(34). Serially passaged HDMECs were plated on gelatin-coated 96-well gold electrode arrays (Applied Bio-Physics, 96W20idfPET). Media (EGM2-MV, Lonza) was changed and TEER measurements recoded daily until HDMECs monolayers reached a plateau that coincided

with maturation of TJ morphology, defined as quiescence(2). To initiate cytokine-induced changes in TEER, TNF was introduced in real time to the media at post-transfection between 48–72 hour. HDMEC monolayer resistances were measured once every 60 seconds by application of a 1μA constant AC current at 4000 Hz between a large and gold electrode embedded in the culture ware. Data was recorded by an ECIS Z-theta instrument controlled by a Dell computer ECIS equipped with ECIS software version 1.2.252 0PC (Applied Biophysics). TEER is reported as the absolute electrical resistance where measured Ohms are divided by the electrode surface area (3.985 mm^2 for 96W20idf PET arrays).

Antibodies and Reagents

Validated TaqMan probes for detecting relative expression of mRNA species: *ARHGEF12* (Thermo Fisher, HS00209661-m1), *GAPDH* (Thermo Fisher, Hs02786624-g1) and *SELE* (Thermo Fisher, Hs00174057-m1) were used. For cell treatments, recombinant human tumor necrosis factor (TNF; Invitrogen, PHC3015), interleukin-1 (IL-1, Invitrogen, A42508) and lipopolysaccharide (LPS, Millipore/Sigma, L4391) were used. For siRNA knockdown of *ARHGEF12*, two composite silencer select siRNAs from Thermo Fischer Scientific (Cat # S-2360 and S-23661), for Rap1A knockdown two composite siRNA from Dharmacon (Sequence: 5'-UGAAGUCGAUUGCCAACAG-3' and 5'-GAACAGAUUUUACGGGUUA-3'), for Rap1B knockdown two composite siRNA from Dharmacon (sequences: 5'-CAGCUGCUUUAAUAUACUA-3' and 5'-AAAAUACGAUCCUACGAUA-3') and for control non-targeting siRNA from Dharmacon (sequence: 5'-UGGUUUACAUGUCGACUAA-3', D-001910–01-05), were used. For siRNA transfection, Lipofectamine RNAiMAX (Applied Biosciences, 13778–150) was used. For immunoblotting, mouse anti-Rap1A monoclonal antibody (Thermo Fisher, MA1–013), rabbit anti-Rap1B polyclonal antibody (Thermo Fisher, PA5–27580), rabbit anti-Rap2A polyclonal antibody (Thermo Fisher, PA5–28905), rabbit anti-Rap2B polyclonal antibody (Thermo Fisher, PA5–30144), rabbit anti-Rap2C polyclonal antibody, rabbit anti-RhoA polyclonal antibody (Abcam, 187027), rabbit anti-RhoB polyclonal antibody (Invitrogen, 711274) rabbit anti-RhoC polyclonal antibody (Abcam, 180785) and mouse anti-beta actin (Sigma, A2228) were used. For single staining immunocytochemistry, polyclonal mouse anti-claudin-5 (Thermo Fisher Scientific, 35–2500), and rabbit anti-ZO-1 (Santa Cruz, SC-33725) and mouse/rabbit IgGs (Invitrogen, Isotype controls) were used. For confocal microscopy, donkey anti-rabbit IgG Alexa Fluor 488 (Thermo Fisher, 21206), donkey anti-mouse IgG Alexa Fluor 546 (Thermo Fisher, A-10036), along with DAPI (Invitrogen) were used to detect primary antibodies. For immunoprecipitation, rabbit anti-ArhGEF12 Polyclonal Antibody (Thermo Fisher, PA5–39418) was used. For Rho A/B/C pulldown, Rho GTPase Activation Assay kits (Cytoskeleton, RT02-A), for Rap isoforms pulldown, active Rap1 pulldown detection kit (Thermo Fisher Scientific, 16120 Y) and for Rac1/Cdc42 pulldown, Rac1/Cdc42 activation assay kit (Cytoskeleton, STA-401–1) were used. For assessing *in vitro* GTP exchange, recombinant human Rap1A protein (Abcam, ab97904), recombinant human Rap1B protein (Abcam ab103049), and Guanosine 5′-Triphosphate, 100 mM solution (Sigma Aldrich, GE27–2076-01) were used.

Confocal Immunofluorescence microscopy

HDMEC monolayers grown on gelatin-coated glass coverslips were washed with phosphate buffered saline (PBS) containing calcium (100 mg/L) and magnesium (100 mg/L) and fixed in 95% ethanol for 30 min at 4°C. For single-color immunofluorescence imaging, monolayers were incubated overnight in either mouse anti–caludin-5 (Thermo Fisher, 4C3C2), or rabbit anti-ZO1 (Santa Cruz, sc-33725) antibodies. Donkey anti-mouse Alexa488 and Donkey anti-rabbit Alexa546 secondary antibodies were used to detect primary antibodies. Glass coverslips were mounted for confocal immunofluorescence analysis in ProLong mounting media with 4′,6-diamidino-2-phenylindole (DAPI, Invitrogen). Randomly selected (minimum of five images per experimental condition) confocal photomicrographs were collected by using a Leica fluorescence microscope (SP5) 63× oil objective (Zeiss) and a digital camera.

Short interfering (si)RNA knockdown of protein expression

HDMECs plated on gelatin-coated (Sigma) 6-well plates (Flacon, Corning) at 50% confluence were transfected with Lipofectamine RNAiMAX (Invitrogen) complexed to two different composite siRNA sequences for each gene deletion that specifically targeted to *ARHGEF12, RAP1A* and *RAP1B*. Cell treatment was done according to the manufacturers protocol. In brief, siRNA complexes of Lipofectamine (Invitrogen) at 50 μg/ml and siRNA at 100 nM were prepared in Opti-MEM reduced serum medium (Invitrogen) and then diluted fivefold in Opti-MEM to yield a final siRNA concentration of 20 nM. The siRNA-Lipofectamine was then added to HDMECs cultures and incubated for 24 hours at 37°C. Fresh medium (EGM-2MV, Lonza) was then added next day, and cells were re-transfected 12 hours later. After resting for 24h, some wells of transfected HDMECs were harvested with trypsin and seeded into gelatin-coated ECIS 96-chamber arrays (Applied Biophysics, 96W20idf PET) at 100,000 cells per well while replicate cultures were used for protein analyses.

Western blotting

HDMECs were lysed in 2x Laemmli buffer (65.8 mM Tris-HCl, pH 6.8, 26.3% (w/v) glycerol, 2.1% SDS, 0.01% bromophenol blue) containing 5% 2-mercaptoethanol. Cell lysates were loaded into each well of SDS gel (Bio Rad) and separated by electrophoresis. For immunoblot analyses, gel was transferred onto Polyvinylidene fluoride (PVDF) membranes (Bio Rad) and blocked with 5% PBS. PVDF membrane was incubated with primary antibodies overnight at 4°C. Secondary antibodies conjugated with HRP or Alexa Fluor 680 were detected with either Super-Signal West Femto ultra-sensitive enhanced chemiluminescent (ECL) substrate (Thermo Scientific) on HyBlot CL autoradiography film (Thermo Fisher) or on LICOR Odyssey CLX, respectively. Immunoblot images display bands of interest and controls from the same contiguous immunoblots with background levels minimized by adjusting all pixels equally with ImageJ 1.52a software (National Institutes of Health). Protein quantification by densitometry was analyzed by using ImageJ(35). The density of the proteins in each control (NT-PBS) group was used as a standard (1 arbitrary unit) to compare the relative density of the other groups.

Pull-down assays of GTP-bound GTPases

Rap1, Rho and Rac1/Cdc42 pulldown assays were performed by using Rap1 activation assay kits (Thermo Fischer, 16120), Rho activation assay kit (Cytoskeleton, RT02-A) and Rac1/Cdc42 activation assay kits (Cytoskeleton, BK034/BK035), respectively, per the manufacturer's protocols. Briefly, HDMECs cultured in C6 plastic wells (Flacon, Corning) were lysed with the buffer contained in the activation assay kits and either frozen in liquid nitrogen or processed immediately. For affinity precipitation of activated Rap1, 500 μL of cell lysates were incubated with 50 μL of glutathione resin slurry in the presence of 10 μg of RalGDS-RBD protein for 1 hour at 4°C. For Rac1/Cdc42 pulldown, 500 μL cell lysates were incubated with PAK-PBD agarose beads with agitation for 1 h at 4°C. For Rho pulldown, 500 μL of cell lysates were incubated with Rhotekin RBD Agarose beads for 1 hour on agitation at 4°C. For RhoA and Rap1A pulldown assay and TNF time course, HDMECs were treated with TNF for 0–12 hours and active RhoA and Rap1A were pulldown with Rhotekin-RBD agarose beads and RalGDS-RBD protein with agitation for 1 hour at 4°C. The beads were pelleted by centrifugation and washed with the kit washing buffer three times. Samples were either frozen at −80°C or processed immediately by mixing with 30 μL of standard SDS-PAGE–reducing Laemmli buffer (Bio-Rad) and placed on a dry bath incubator (Fisher Scientific) for 5 min at 95C and run on protein gel electrophoresis.

ArhGEF12 immuno-isolation and cell-free functional assays

Immunoprecipitation of ArhGEF12 protein was performed with protein A/G Sepharose bead immunoprecipitation kit (Abcam, ab206996) per the manufacturers protocol. HDMECs cultured in T75 were PBS washed twice and lysed with cold non-denaturing lysis buffer. Scrapped cell lysate was gently transferred into a chilled microcentrifuge tube followed by mixing on rotary for 30 minutes at 4°C. Anti-ArhGEF12 or anti-IgG isotype control (6 μg/mg) was added to the cell lysate sample (500 μg/mL) and mixed overnight on rotary at 4°C. After antibody binding, 25–40 μL of protein A/G Sepharose beads were added to each tube and incubated for 1 hour at 4°C. Protein A/G Sepharose beads were collected by low centrifugation (200 x g for 2 minutes) and washed three times. To detect effective pulldown of ArhGEF12, SDS-PAGE–reducing Laemmli buffer (Bio-Rad) was added to a small separate 20 μL aliquot of beads and boiled for 5 minutes and then frozen or immediately processed for Western blot analysis as described above. To assess function, protein A/G Sepharose beads binding ArhGEF12 were suspended in 50 μL of buffer (125 mM HEPES, 750 mM NaCl, 50 mM $MgCl_2$, 5 mM EDTA, 10 5 glycerol, and 5% NP-40) in the presence of GTP (1mM) and recombinant Rap1A/B proteins (Abcam) and incubated for 30 minutes at 37°C. GTP loaded active Rap1 proteins were pulled-down with RalGDS-RBD pull-down assays as described above. Samples were either frozen at −80°C or processed immediately by mixing with 30 μL of standard SDS-PAGE–reducing Laemmli buffer (Bio-Rad) and placed on a dry bath incubator (Fisher Scientific) for 5 min at 95–100°C and then subjected to protein gel electrophoresis.

Statistics

Results are expressed as means with standard deviations. Statistical analyses were performed by using GraphPad Prism software (V9.2.0 GraphPad). Ordinary one-way analysis of

variance (ANOVA) tests were performed to compare two groups, two-way ANOVA tests were performed to compare multiples groups, paired t-tests and non-parametric Mann-Whitney tests were used for multiple comparisons with two or more groups (n=3). A $p < 0.05$ was considered statistically significant.

RESULTS

ARHGEF12 is differentially regulated in cultured tight junction forming human dermal microvascular endothelial cells (HDMECs) compared to human umbilical vein endothelial cells (HUVECs)

We hypothesized that GEFs which antagonize TNF effects on ECs might be downregulated by TNF treatment and that a GEF relevant for regulating TJ-dependent capillary barrier function could be differentially regulated in HDMECs compared to HUVECs. To identify genes that are specifically downregulated in HDMECs during inflammation, we carried out whole transcriptome analysis of cultured ECs, with and without TNF treatment. Of the 73 known GEFs, 57 were significantly differentially expressed between TNF and saline conditions with 25 GEFs were significantly downregulated by TNF stimulation (false discovery rate, $q<0.05$). Using comparative analysis of whole transcriptome analysis of HDMECs (GSE161021) and HUVECs (GSE190181) under the same culture conditions, we identified only *ARHGEF12* as being more highly expressed in HDMECs compared to HUVECs in unstimulated culture conditions (Table 1, q=0.000163). Additionally, *ARHGEF12* is significantly downregulated in TNF-treated HDMECs but unchanged in HUVECs under the same conditions (Table 1, q=0.000163 and 0.678816 respectively). HDMECs and HUVECs may also predominately express different isoforms of ArhGEF12 (202 vs. 201, respectively). Concordant with a decline in *ARHGEF12* mRNA expression, ArhGEF12 protein is decreased in HDMECs by 6 hours after TNF treatment (Figure 1A). Although IL-1 and LPS produce similar disruption of TJs in HDMEC monolayers, *ARHGEF12* expression is unchanged in HDMECs six hours after treatment with IL-1 and is somewhat increased after treatment with LPS (Supplemental Figure 1A). Disruption of TJs involves the activation of NF-κB signaling. However, the TNF-mediated decrease in *ARHGEF12* expression was only partly mitigated by inhibition of NF-κB activation by Bay11–7085 (Bay11, Supplemental Figure 1A). In the same cultures, Bay11 strongly inhibited induction of *SELE,* which encodes for E-selectin, a TNF-induced transcript dependent on NF-κB (Supplemental Figure 1B) indicating successful inhibition.

ArhGEF12 depletion significantly exacerbates TNF induced decrease in trans-endothelial electrical resistance (TEER).

To determine if and how ArhGEF12 affects TNF-induced endothelial permeability, we reduced its expression in HDMECs by siRNA knock down and analyzed its effects on trans-endothelial electrical resistance (TEER). Both mRNA (Figure 1B) and protein levels (Figure 1C) were reduced by more than 90% with siRNA treatment. HDMECs depleted of ArhGEF12 remain capable of forming normal barriers as indicated by similar levels TEER prior to addition of TNF (Figure 1D, 0-hour timepoint). Strikingly, depletion of ArhGEF12 produced more rapid and significantly increased disruption of barrier function after low dose TNF stimulation (1 ng/mL, Figure 1D).

Depletion of ArhGEF12 disrupt TJ architecture in TNF stimulated HDMECs

Changes in paracellular permeability in HDMECs are associated with characteristic disruption of TJ proteins such as claundin-5 and zona occludens-1 (ZO-1)(36, 37). Immunofluorescence confocal microscopy of non-targeting (NT) and *ARHGEF12* targeting siRNA transfected HDMECs treated with PBS display smooth and continuous junctional staining for claudin-5 (Green) and ZO-1 (Red) (Fig 2A, top panels #2 and #4, white arrows), indicative of normal TJ architecture. In contrast, HDMECs stimulated with TNF for 6 hours demonstrate disruption of TJ protein organization (Fig 2A, quantification B, C). Both HDMECs transfected with *ARHGEF12* siRNA display significantly more disorganized claudin-5 and ZO-1 staining in a characteristic “saw-tooth” pattern when treated with TNF for 6 hours, suggesting TJ protein disruption (Fig 2A lower panels #2 and #4, yellow arrows). However, HDMECs transfected with non-targeting (NT) siRNA and TNF display less disrupted junctions, with preserved junctional segments of smooth and continuous staining of claudin-5 and ZO-1 (Fig. 2A, lower panel #1 and #3), quantified by measuring the proportion of the circumferential smooth, confluent staining around individual cells to the total cellular circumference. In the PBS-treated cells, there is greater than 80% continuity of circumferential staining in all groups (Fig 2 B, C, PBS groups). HDMECs treated with *ARHGEF12* siRNA and TNF show more significant disruption of confluent staining (Fig 2 B, C, TNF groups), the effect of TNF appears greater than that observed in HDMECs transfected with NT siRNA (Fig 2 B, C, TNF groups). These results demonstrate depletion of ArhGEF12 exacerbates disruption of claudin-5 and ZO-1 junctional organization after 6 hours of TNF stimulation, consistent with ECIS measurements indicating a more pronounced paracellular leak at that timepoint.

Rap1A is activated by TNF in HDMECs and ArhGEF12 depletion selectively reduces levels of active Rap1A.

To determine a mechanism by which ArhGEF12 could stabilize TJs, we sought to identify its effector GTPase target. Rac1 and Cdc42 are the best described GTPases that act to promote barrier function and improve junctional stability in ECs(38). We utilized pull-down assays to selectively detect levels of active GTP-bound Rac1/Cdc42 in HDMEC lysates. ArhGEF12 depletion does not change the amount of active Rac1 or Cdc42 after TNF stimulation (Supplemental Figures 2A, B quantification C-F), suggesting that ArhGEF12 does not activate either of these GTPases.

ArhGEF12 has previously been identified as a GEF for RhoA, first in leukemia cells(39) and subsequently in HUVECS(40–42), predominantly activated in response to mechanical stimulation. Active RhoA functions to decrease endothelial barrier function(43), which would predict the opposite of the effect we observed upon knock down of ArhGEF12. To determine if and when RhoA is activated by TNF in HDMECs, we performed serial pull-down assays after stimulation demonstrating significantly increased GTP loading by 8 hours (Figure 3A, quantification B, C). ArhGEF12 depletion paradoxically results in significantly sustained activation of RhoA by 12 hours after TNF. ArhGEF12 depletion does not alter activity of RhoB or RhoC after TNF stimulation (Supplementary Figure 3A, B, quantification C-F).

The apparent role played by ArhGEF12 in antagonizing TNF-induced TJ disruption led us to consider other potential targets of this GEF that might stabilize the barrier. Rap1 is established to promote barrier function but the specific effects of Rap1A and Rap1B in TJ-forming ECs are not defined(44). Serial activity assays demonstrate Rap1A is maximally GTP-loaded by eight hours after TNF treatment. Active Rap1A levels are significantly decreased by ArhGEF12 depletion as early as four hours after TNF treatment relative to total Rap1A and β-actin (Figure 3D, quantification E, F). Conversely, levels of active Rap1B are not significantly different before or eight hours after TNF treatment in either NT-treated or ArhGEF12 depleted HDMECs (Fig. 4A, B). The proportional decrease in active Rap1A compared to no change in active Rap1B suggests that ArhGEF12 could be a GEF that specifically activates only Rap1A in intact HDMECs (Fig. 4A, B quantification C-F). Depletion of ArhGEF12 does not alter the GTP loading of Rap2A-C proteins eight hours after TNF stimulation (Supplemental Figure 4A-C, quantification D-I).

ArhGEF12 isolated from HDMECs acts as a GEF for both recombinant Rap1A and RhoA *in vitro.*

To determine the specificity of ArhGEF12 for Rap1A, Rap1B and RhoA, we tested the interactions of ArhGEF12 with different recombinant GTPases in cell free assays. We immuno-isolated ArhGEF12 from HDMEC cell lysates and incubated with individual recombinant Rap1A, RhoA and Rap1B in the presence of exogenous GTP (Fig.5 A, C, E, quantification G-I). After incubation, we carried out pulldown activity assays and immunoblotting and determined the extent of GTP loading. Rap1A GTP loading is dramatically increased by ArhGEF12 (Fig.5 B, quantification J) showing that ArhGEF12 is a functional GEF for Rap1A. As expected from the literature, ArhGEF12 is also able to load GTP on to RhoA (Fig. 5F, quantification L). Notably, ArhGEF12 does not catalyze GTP loading onto Rap1B (Fig 5D, quantification K) nor onto RhoB or RhoC (Supplemental Figure 5).

DISCUSSION

Capillary leak due to acute and overwhelming inflammation is a core pathophysiologic feature of clinical entities such as septic shock or post-cardiac arrest multi-organ failure. Care for these patients is challenging, and therapies are limited to intensive supportive care, due in large part to our lack of understanding of how the TJ-dependent capillary barrier is restored. A focus on the capillary segment is essential; while venular leak may be physiologic, capillary leak is always pathologic and resultant organ edema produces tissue dysoxia, worsening organ failure. In this study, we have used cultured HDMEC rather than the more widely used HUVEC cultures to study TNF-induced disruption of TJs in ECs. Our HDMEC cultures include several different types of skin ECs derived from different microvascular segments of both the blood and lymphatic microvasculature. However, once in culture, they acquire a new phenotype, behaving uniformly. For example, despite expression of lymphatic markers Prox1 and podoplanin, 100% of our cultured HDMECs express E-selectin upon treatment with TNF, something that is seen primarily in blood post-capillary venules and not typically observed in skin lymphatic ECs in situ(45). Moreover, our cultured HDMECs produce basement membrane proteins such as collagen

IV, characteristic of blood rather than lymphatic ECs. We have previously described that human arterial and venous ECs also converge to a common cell EC phenotype after less than 72 h in culture(46).Our rationale for investigating specific GEFs in HDMECs compared to HUVECs is that, unlike HUVECs, HDMECs spontaneously form ZO-1/claudin 5-organized TJs under standard culture conditions, detected morphologically and functionally, that are not dependent upon calcium or VE-cadherin for their integrity and that this spontaneous process may depend of the action of specific GEFs. As we have reported previously, HUVECs at confluence do synthesize ZO-1 and claudin 5, but under the same standard culture conditions, HUVECs do not assemble these proteins into morphological TJs and their intercellular junctions remain as low resistance barriers formed by calcium-dependent VE-cadherin-based AJs(2). While it is possible to induce HUVECs to form TJs by means of pharmacological agents that raise cAMP levels combined with astrocyte-conditioned medium, this creates an increasingly non-physiological setting for studying TJ disruption in peripheral tissues(2). We use ECIS to allow continuous monitoring of HDMEC junctional integrity that has been found to correlate with assays of macromolecular flux, with the advantage of permitting time resolved changes in barrier function(12). TNF stimulation reliably disrupts TJ function and architecture in HDMECs. Utilizing this culture model and methods of analyses, our major finding is that ArhGEF12 acts as a highly selective activator of Rap1A, and not RhoA or Rap1B, serving to counter TJ disruption in the setting of TNF-induced paracellular leak.

We identified *ARHGEF12* using transcriptional screening of uniquely regulated GEFs in HDMECs compared to HUVECs. Our results demonstrate transcriptional control of GAPs and GEFs are significant to cellular function and adaptation to stimulation. Identifying the mechanisms underlying TNF downregulation of ArhGEF12 are critically important. Prior work demonstrated that TNF-mediated disruption of TJs in cultured HDMECs was dependent upon activation of NF-κB signaling. We demonstrate that other proinflammatory agents that similarly act through NF-κB signaling (IL-1 and LPS) to disrupt TJ barriers do not significantly decrease *ARHGEF12* expression. In fact, treatment with LPS significantly increases ARHGEF12 expression, with and without NF-κB inhibition (Supplemental Figure 1A). The TNF-induced fall in *ARHGEF12* expression level is minimally reduced by NF-κB inhibition, suggesting *ARHGEF12* is downregulated independent of NF-κB activation. This may be due to other TNF receptor 1 (TNFR1) signaling pathways or signaling through TNFR2(47, 48). The observed differential expression of *ARHGEF12* between HDMECs and HUVECs may involve expression of different isoforms (HUVECs mainly express 201 while HDMECs express 202). However, both of these isoforms are believed to be produced from mRNAs initiated from the same transcriptional start site, suggesting that inhibition of transcription is unlikely to be the explanation for the TNF effect. Another possible mechanism of TNF mediated reduction in expression in HDMECs may be post transcriptional, e.g. by microRNA (miR) expression(49) or long non-coding RNAs (lncRNA)(50). Established in pulmonary artery smooth muscle cells, miR-214 is known to regulate *ARHGEF12* expression. We do not detect miR-214 in our bulk RNAseq analysis, although mature miRs may not be captured due to their small size. Longer miRs, and lncRNA such as miR-22, are differentially expressed and are predicted to interact with *ARHGEF12* (GSE190181)(51). In fact, a comparison of our bulk RNAseq HDMECs vs.

HUVECs both stimulated with TNF we identify many significantly differentially regulated longer miRs and lncRNAs (Supplemental Table 1). This analysis may lack sensitivity for smaller miRs. Targeted miR analysis and identification of the genetic and/or epigenetic regulation of *ARHGEF12* between HDMECs and HUVECs is an important focus of future research that may have relevance to how other GAPs and GEFs are regulated in the setting of endothelial cellular stress such as acute critical illness.

Here we focus on how changes in ArhGEF12 expression in HDMECs functionally impact the TJ-dependent barrier. ECIS assays on genetically modified EC provides an efficient way to rapidly untangle the functional effects of the complicated and many times overlapping GAP/GEF/GTPase signaling cascades. These results are supported by examining the organization of the TJ proteins, claudin-5 and ZO-1 and ultimately activity of specific GTPases in intact HDMEC and in cell-free assays. This combined approach can identify and assign new functional specificity to GAPs and GEFs.

Multiple GTPases are known to increase endothelial barrier function. Perhaps the best studied are Rac1 and Cdc42, which have known GEFs of promiscuous specificity such as Trio and Tiam1(52), GEF-H1(53), Vav2(54), Tuba(55) and others(56). We demonstrate that ArhGEF12 does not activate either Rac1 or Cdc42 in HDMECs stimulated with TNF. ArhGEF12 has been described to activate RhoA in a variety of non-capillary cell types(57–59) as well as in HUVECs, predominately in the setting of a response to cell shear stress(40–42). ArhGEF12/RhoA interactions have not been investigated in endothelial cells in the setting of inflammatory stimulation. RhoA is thought to decrease endothelial barrier function(60), inconsistent with our observed phenotype in ArhGEF12 depleted HDMEC. None of these functions have been investigated in TJ-forming ECs.

Precise cellular regulation of GEF activity is essential due to the wide range of downstream cellular effects and ability to amplify signal transduction(61). We demonstrate unique cellular specificity of ArhGEF12 for Rap1A and not RhoA in HDMECs (Figure 3) with promiscuous RhoA activation in cell free assays (Figure 5), suggesting ArhGEF12 has the ability, but not opportunity, to activate RhoA in HDMECs. Indeed, loss of ArhGEF12 paradoxically results in increased RhoA activity in HDMECs. In intact cells, such specificity may be accomplished by restricted subcellular location(62), post-translational protein stability or competition with higher affinity binding partners. The former is well established for Rho-GTPases by post-translational fatty acid modification(63), association with guanine dissociation inhibitors(64) and sequestration in specific intracellular compartments(65). Many GAPs and GEFs are predicted to have promiscuous substrate specificity(66), and depletion of ArhGEF12 may allow more efficient binding of a different GEF to RhoA but not Rap1A. We also demonstrate ArhGEF12 does not have activity on any Rap2 isoforms, which is consistent with our observed TEER results. Rap2 depletion in HUVECs increases TEER with no specifically identified effects of individual isoforms, suggesting redundant, barrier-destabilizing effects for Rap2A-C(15). Such effects may be mediated through MAP4K4 signaling and actin disruption by Ste20 kinases(67),. PDZ-GEF1 and 2, encoded by *RAPGEGF2* and *RAPGEF6* respectively, act as GEFs to activate Rap2 isoforms(68, 69), however these also act as GEFs for Rap1, suggesting overlapping and antagonistic signaling(70). Similar to RhoA, ArhGEF12 activating Rap2 isoforms would not

match our observed TEER phenotype, and no activity was observed in our analysis of cell lysates.

Perhaps most striking, utilizing cell free assays, we demonstrate that immuno-isolated ArhGEF12 is highly selective for Rap1A and not Rap1B (Figure 5). Despite human Rap1A and Rap1B differing by only nine amino acids, ArhGEF12 does not catalyze GTP loading to Rap1B but does onto RhoA, with which Rap1A shares 30% sequence identity (Figure 6) (71). Although extensively investigated, the regulation of Rap1 remains somewhat indistinct due to the paucity of studies focusing specifically on Rap1A. Initial studies collectively suggested Rap1A and -B to be activated by the cAMP-responsive GEF Epac1 (encoded by *RAPGEF3(21)*) and PDZ-GEF (*RAPGEF2*)(72). Subsequent seminal studies focused specifically on Rap1A without parallel investigations of Rap1B, and established activation by cAMP-GEFI and cAMP-GEFII (*RAPGEF2* and *RAPGEF4*) in neurons(73) or RAS Guanyl Releasing Protein 2 (*RASGRP2*) in platelets(74). In total, six major classes of GEFs have been implicated in Rap1 activation: C3G (*RAPGEF1*), PDZ-GEFs (*RAPGEF2*,*−6*), Epac proteins (*RAPGEF3,−4,−5*), RasGRP isoforms (*RASGRP2,−3*), a GEF domain in phospholipase C epsilon (*PLCE1*) and dedicator of cytokinesis 4 (*DOCK4*)(75). Given the high sequence identity between Rap1A and -B, it's not surprising that, when tested, these GEFs activate both Rap1A and Rap1B. No prior reports have implicated a GEF specific for Rap1A but not Rap1B nor has any RhoGEF been previously known to activate Rap1A. The majority of these investigations were performed in other cell types and, to our knowledge, ArhGEF12 is the first identified Rho-GEF able to activate Rap1A but not Rap1B and that it does so in capillary ECs.

An unexpected finding was that depletion of ArhGEF12 paradoxically resulted in *increased* RhoA activity, predominately at later timepoints (Figure 3B,C). The reasons for increased RhoA activity in the ArhGEF12 depleted HDMECs are not obvious. One possible explanation is that the absence of ArhGEF12 allows other GEFs to physically access to RhoA. Proximity interaction analysis predicts multiple potential RhoA-GEFs, many of which have been previously experimentally verified in different culture systems(76). Many of these promiscuous RhoA-GEFs, namely the above-mentioned Trio and Vav2, are expressed in HDMECs and significantly upregulated after TNF stimulation (Supplemental Table 2).

The downstream effects of Rap1 activation have been extensively studied in ECs, notably via Epac1 activity, with most of these studies not focused on the functional contributions of specific isoforms. Collectively, Rap1 activation is known to enhance barrier function through FGD5-mediated activation of Cdc42 and separate Radil/Rasip1 and KRIT1 mediated inhibition of Rho Associated Coiled-Coil Containing Protein Kinase 1 (ROCK1) activity(77). A single study suggested Rap1A may differentially promote adherens junctions formation in HUVECs(18), but this study did not focus on TJs nor barrier restoration in the setting of inflammation. ROCK1 activity is established to increase cellular tension and breakdown TJ-dependent EC barriers(78). We demonstrate differential isoform activity where Rap1A is critical for TJ-dependent barrier restoration after inflammation induced leak while Rap1B is not. A potential mechanism for this effect could be that Rap1A functions to activate Rac1 through binding to Vav2 and Tiam1(79), both known GEFs for Rac1(80).

Another potential mechanism would be reduction of ROCK1 activity in HDMEC. Finally, modulation of AJs by Rap1A may be a critical intermediary step as the formation of TJs depends on the presence of AJs. Epac1-Rap1A activity is noted to increase cortical actin(81), promote microtubule growth(82) and increase the number and stability of AJs in cultured endothelial cells(83). These processes may establish more AJs available to promote TJ formation specifically after disruption with pro-inflammatory cytokines. These hypotheses require testing in future work with a focus on the *in vivo* ramifications of Rap1A activation.

In conclusion, we demonstrate that differential transcriptional profiling of TJ-forming ECs reveals distinct transcriptional regulation of ArhGEF12. Functional studies of this protein in HDMECs show it to be a specific GEF for Rap1A, and not Rap1B or RhoA, that functions to limit disruption of TJ- dependent barriers induced by TNF.

Supplementary Material

Refer to Web version on PubMed Central for supplementary material.

ACKNOWLEDGEMENTS

We would like to thank Yale's Department of Pediatrics and the Vascular Biology and Therapeutics Program for ongoing support and thank HPC facilities at Yale Center for Research Computing and the Yale Center for Genome Analysis.

SOURCES OF FUNDING

This work has been supported by grants from the Charles H. Hood Foundation, NIH/NHLBI 1K08HL136898–01A1, NIH/NICHD K12HD047349, NIH/NHLBI 5 T32 HL 7974–19, NIH 1S10OD018521–01

DATA AVAILABILITY STATEMENT

Bulk RNA-sequencing data before and after stimulation with tumor necrosis factor used in this manuscript were generated using cultured human umbilical venous endothelial cells (HUVEC) and human dermal microvascular endothelial cells (HDMEC). HUVEC are commercially available from Yale's Vascular Biology and Therapeutics (VBT) program (https://medicine.yale.edu/vbt/order/). HDMEC are isolated using published protocols and are available from the Corresponding Author upon request. The comparative bulk RNA-sequencing data that support the findings of this study are openly available at NCBI's Gene Expression Omnibus (https://www.ncbi.nlm.nih.gov/geo/) for both HDMEC (GSE161021) and HUVEC (GSE190181). All other data were generated using commercially available and validated reagents as described in the manuscript. Data is processed using commercially available programs as described.

Non-standard Abbreviations and Acronyms

AJ	Adherens junctions
ARHGEF12	Rho guanine nucleotide exchange factor 12
EC	Endothelial cell

ECIS	Electrical cell-substrate impedance sensing
EGM-2 MV	Microvascular endothelial cell growth medium-2
GAP	GTPase activating protein, also known as GTPase-accelerating proteins
GEF	Guanine nucleotide exchange factor
HDMEC	Human dermal microvascular endothelial cells
HUVECs	Human umbilical vascular endothelial cells
IP	Immunoprecipitation
NF-κB	Nuclear factor kappa-light-chain-enhancer of activated B cells
NT	Non-targeting
PBS	Phosphate buffered saline
RalGDS-RBD	Ral guanine nucleotide dissociation stimulator for Rap-binding domain
ROCK	Rho-Associated Coiled-Coil Kinase
TEER	Trans-endothelial electrical resistance
TJ	Tight junction
TNF	Tumor necrosis factor
ZO1	Zona occludens-1

REFERENCES

1. Pierce RW, Giuliano JS Jr., and Pober JS (2017) Endothelial Cell Function and Dysfunction in Critically Ill Children. Pediatrics 140, 11
2. Kluger MS, Clark PR, Tellides G, Gerke V, and Pober JS (2013) Claudin-5 controls intercellular barriers of human dermal microvascular but not human umbilical vein endothelial cells. Arterioscler Thromb Vasc Biol 33, 489–500 [PubMed: 23288152]
3. Duong CN, and Vestweber D (2020) Mechanisms Ensuring Endothelial Junction Integrity Beyond VE-Cadherin. Front Physiol 11, 519 [PubMed: 32670077]
4. Pober JS, and Sessa WC (2014) Inflammation and the blood microvascular system. Cold Spring Harb Perspect Biol 7, a016345 [PubMed: 25384307]
5. Redl H, Dinges HP, Buurman WA, Linden C. J. v. d., Pober JS, Cotran RS, and Schlag G (1991) Expression of endothelial leukocyte adhesion molecule-1 in spetic but not traumatic/hypovolemic shock in the baboon. American Journal of Pathology 139, 461–466 [PubMed: 1714243]
6. Zancanaro A, Serafini F, Fantin G, Murer B, Cicardi M, Bonanni L, Dalla Vestra M, Scanferlato M, Mazzanti G, and Presotto F (2015) Clinical and pathological findings of a fatal systemic capillary leak syndrome (Clarkson disease): a case report. Medicine (Baltimore) 94, e591 [PubMed: 25738482]
7. Cherfils J, and Zeghouf M (2013) Regulation of small GTPases by GEFs, GAPs, and GDIs. Physiol Rev 93, 269–309 [PubMed: 23303910]

8. Bos JL, Rehmann H, and Wittinghofer A (2007) GEFs and GAPs: critical elements in the control of small G proteins. Cell 129, 865–877 [PubMed: 17540168]
9. Spindler V, Schlegel N, and Waschke J (2010) Role of GTPases in control of microvascular permeability. Cardiovasc Res 87, 243–253 [PubMed: 20299335]
10. Marcos-Ramiro B, Garcia-Weber D, Barroso S, Feito J, Ortega MC, Cernuda-Morollon E, Reglero-Real N, Fernandez-Martin L, Duran MC, Alonso MA, Correas I, Cox S, Ridley AJ, and Millan J (2016) RhoB controls endothelial barrier recovery by inhibiting Rac1 trafficking to the cell border. J Cell Biol 213, 385–402 [PubMed: 27138256]
11. Pierce R, Merola J, Lavik LP, Kluger M, Hufner A, Khokha M, and Pober J (2017) A Mutation in p190BRhoGAP Prolongs RhoB Activation and May Explain a Fatal Systemic Capillary Leak Syndrome. Journal of Experimental Medicine In revsion
12. Khan A, Ni W, Lopez-Giraldez F, Kluger MS, Pober JS, and Pierce RW (2021) Tumor necrosis factor-induced ArhGEF10 selectively activates RhoB contributing to human microvascular endothelial cell tight junction disruption. FASEB J 35, e21627 [PubMed: 33948992]
13. Rousseau-Merck MF, Pizon V, Tavitian A, and Berger R (1990) Chromosome mapping of the human RAS-related RAP1A, RAP1B, and RAP2 genes to chromosomes 1p12----p13, 12q14, and 13q34, respectively. Cytogenet Cell Genet 53, 2–4 [PubMed: 2108841]
14. van Dam TJ, Bos JL, and Snel B (2011) Evolution of the Ras-like small GTPases and their regulators. Small GTPases 2, 4–16 [PubMed: 21686276]
15. Pannekoek WJ, Linnemann JR, Brouwer PM, Bos JL, and Rehmann H (2013) Rap1 and Rap2 antagonistically control endothelial barrier resistance. PLoS One 8, e57903 [PubMed: 23469100]
16. Li Y, Yan J, De P, Chang HC, Yamauchi A, Christopherson KW 2nd, Paranavitana NC, Peng X, Kim C, Munugalavadla V, Kapur R, Chen H, Shou W, Stone JC, Kaplan MH, Dinauer MC, Durden DL, and Quilliam LA (2007) Rap1a null mice have altered myeloid cell functions suggesting distinct roles for the closely related Rap1a and 1b proteins. J Immunol 179, 8322–8331 [PubMed: 18056377]
17. Chrzanowska-Wodnicka M, White GC 2nd, Quilliam LA, and Whitehead KJ (2015) Small GTPase Rap1 Is Essential for Mouse Development and Formation of Functional Vasculature. PLoS One 10, e0145689 [PubMed: 26714318]
18. Wittchen ES, Aghajanian A, and Burridge K (2011) Isoform-specific differences between Rap1A and Rap1B GTPases in the formation of endothelial cell junctions. Small GTPases 2, 65–76 [PubMed: 21776404]
19. Lakshmikanthan S, Sobczak M, Li Calzi S, Shaw L, Grant MB, and Chrzanowska-Wodnicka M (2018) Rap1B promotes VEGF-induced endothelial permeability and is required for dynamic regulation of the endothelial barrier. J Cell Sci 131
20. Chen H, Tsalkova T, Chepurny OG, Mei FC, Holz GG, Cheng X, and Zhou J (2013) Identification and characterization of small molecules as potent and specific EPAC2 antagonists. J Med Chem 56, 952–962 [PubMed: 23286832]
21. de Rooij J, Zwartkruis FJ, Verheijen MH, Cool RH, Nijman SM, Wittinghofer A, and Bos JL (1998) Epac is a Rap1 guanine-nucleotide-exchange factor directly activated by cyclic AMP. Nature 396, 474–477 [PubMed: 9853756]
22. Kluger MS, Shiao SL, Bothwell AL, and Pober JS (2002) Cutting Edge: Internalization of transduced E-selectin by cultured human endothelial cells: comparison of dermal microvascular and umbilical vein cells and identification of a phosphoserine-type di-leucine motif. J Immunol 168, 2091–2095 [PubMed: 11859093]
23. Burns AR, Walker DC, Brown ES, Thurmon LT, Bowden RA, Keese CR, Simon SI, Entman ML, and Smith CW (1997) Neutrophil transendothelial migration is independent of tight junctions and occurs preferentially at tricellular corners. J Immunol 159, 2893–2903 [PubMed: 9300713]
24. Burns AR, Bowden RA, MacDonell SD, Walker DC, Odebunmi TO, Donnachie EM, Simon SI, Entman ML, and Smith CW (2000) Analysis of tight junctions during neutrophil transendothelial migration. J Cell Sci 113 **(**Pt 1**)**, 45–57 [PubMed: 10591624] **()**
25. Beese M, Wyss K, Haubitz M, and Kirsch T (2010) Effect of cAMP derivates on assembly and maintenance of tight junctions in human umbilical vein endothelial cells. BMC Cell Biol 11, 68 [PubMed: 20822540]

26. McRae M, LaFratta LM, Nguyen BM, Paris JJ, Hauser KF, and Conway DE (2018) Characterization of cell-cell junction changes associated with the formation of a strong endothelial barrier. Tissue Barriers 6, e1405774 [PubMed: 29388870]
27. Birukova AA, Zebda N, Fu P, Poroyko V, Cokic I, and Birukov KG (2011) Association between adherens junctions and tight junctions via Rap1 promotes barrier protective effects of oxidized phospholipids. J Cell Physiol 226, 2052–2062 [PubMed: 21520057]
28. Siddharthan V, Kim YV, Liu S, and Kim KS (2007) Human astrocytes/astrocyte-conditioned medium and shear stress enhance the barrier properties of human brain microvascular endothelial cells. Brain Res 1147, 39–50 [PubMed: 17368578]
29. Kim D, Langmead B, and Salzberg SL (2015) HISAT: a fast spliced aligner with low memory requirements. Nat Methods 12, 357–360 [PubMed: 25751142]
30. Pertea M, Pertea GM, Antonescu CM, Chang TC, Mendell JT, and Salzberg SL (2015) StringTie enables improved reconstruction of a transcriptome from RNA-seq reads. Nat Biotechnol 33, 290–295 [PubMed: 25690850]
31. Harrow J, Frankish A, Gonzalez JM, Tapanari E, Diekhans M, Kokocinski F, Aken BL, Barrell D, Zadissa A, Searle S, Barnes I, Bignell A, Boychenko V, Hunt T, Kay M, Mukherjee G, Rajan J, Despacio-Reyes G, Saunders G, Steward C, Harte R, Lin M, Howald C, Tanzer A, Derrien T, Chrast J, Walters N, Balasubramanian S, Pei B, Tress M, Rodriguez JM, Ezkurdia I, van Baren J, Brent M, Haussler D, Kellis M, Valencia A, Reymond A, Gerstein M, Guigo R, and Hubbard TJ (2012) GENCODE: the reference human genome annotation for The ENCODE Project. Genome Res 22, 1760–1774 [PubMed: 22955987]
32. Love MI, Huber W, and Anders S (2014) Moderated estimation of fold change and dispersion for RNA-seq data with DESeq2. Genome Biol 15, 550 [PubMed: 25516281]
33. Benjamini Y, Drai D, Elmer G, Kafkafi N, and Golani I (2001) Controlling the false discovery rate in behavior genetics research. Behav Brain Res 125, 279–284 [PubMed: 11682119]
34. Lo CM, Keese CR, and Giaever I (1995) Impedance analysis of MDCK cells measured by electric cell-substrate impedance sensing. Biophys J 69, 2800–2807 [PubMed: 8599686]
35. Schneider CA, Rasband WS, and Eliceiri KW (2012) NIH Image to ImageJ: 25 years of image analysis. Nat Methods 9, 671–675 [PubMed: 22930834]
36. Clark PR, Kim RK, Pober JS, and Kluger MS (2015) Tumor necrosis factor disrupts claudin-5 endothelial tight junction barriers in two distinct NF-kappaB-dependent phases. PLoS One 10, e0120075 [PubMed: 25816133]
37. Sim X, Jensen RA, Ikram MK, Cotch MF, Li X, MacGregor S, Xie J, Smith AV, Boerwinkle E, Mitchell P, Klein R, Klein BE, Glazer NL, Lumley T, McKnight B, Psaty BM, de Jong PT, Hofman A, Rivadeneira F, Uitterlinden AG, van Duijn CM, Aspelund T, Eiriksdottir G, Harris TB, Jonasson F, Launer LJ, Wellcome Trust Case Control, C., Attia J, Baird PN, Harrap S, Holliday EG, Inouye M, Rochtchina E, Scott RJ, Viswanathan A, Global BC, Li G, Smith NL, Wiggins KL, Kuo JZ, Taylor KD, Hewitt AW, Martin NG, Montgomery GW, Sun C, Young TL, Mackey DA, van Zuydam NR, Doney AS, Palmer CN, Morris AD, Rotter JI, Tai ES, Gudnason V, Vingerling JR, Siscovick DS, Wang JJ, and Wong TY (2013) Genetic loci for retinal arteriolar microcirculation. PLoS One 8, e65804 [PubMed: 23776548]
38. Cerutti C, and Ridley AJ (2017) Endothelial cell-cell adhesion and signaling. Exp Cell Res 358, 31–38 [PubMed: 28602626]
39. Reuther GW, Lambert QT, Booden MA, Wennerberg K, Becknell B, Marcucci G, Sondek J, Caligiuri MA, and Der CJ (2001) Leukemia-associated Rho guanine nucleotide exchange factor, a Dbl family protein found mutated in leukemia, causes transformation by activation of RhoA. J Biol Chem 276, 27145–27151 [PubMed: 11373293]
40. Takefuji M, Kruger M, Sivaraj KK, Kaibuchi K, Offermanns S, and Wettschureck N (2013) RhoGEF12 controls cardiac remodeling by integrating G protein- and integrin-dependent signaling cascades. J Exp Med 210, 665–673 [PubMed: 23530122]
41. Lessey-Morillon EC, Osborne LD, Monaghan-Benson E, Guilluy C, O'Brien ET, Superfine R, and Burridge K (2014) The RhoA guanine nucleotide exchange factor, LARG, mediates ICAM-1-dependent mechanotransduction in endothelial cells to stimulate transendothelial migration. J Immunol 192, 3390–3398 [PubMed: 24585879]

42. Abiko H, Fujiwara S, Ohashi K, Hiatari R, Mashiko T, Sakamoto N, Sato M, and Mizuno K (2015) Rho guanine nucleotide exchange factors involved in cyclic-stretch-induced reorientation of vascular endothelial cells. J Cell Sci 128, 1683–1695 [PubMed: 25795300]
43. Wojciak-Stothard B, Entwistle A, Garg R, and Ridley AJ (1998) Regulation of TNF-alpha-induced reorganization of the actin cytoskeleton and cell-cell junctions by Rho, Rac, and Cdc42 in human endothelial cells. J Cell Physiol 176, 150–165 [PubMed: 9618155]
44. Pannekoek WJ, Post A, and Bos JL (2014) Rap1 signaling in endothelial barrier control. Cell Adh Migr 8, 100–107 [PubMed: 24714377]
45. Groger M, Niederleithner H, Kerjaschki D, and Petzelbauer P (2007) A previously unknown dermal blood vessel phenotype in skin inflammation. J Invest Dermatol 127, 2893–2900 [PubMed: 17882274]
46. Liu M, Kluger MS, D'Alessio A, Garcia-Cardena G, and Pober JS (2008) Regulation of arterial-venous differences in tumor necrosis factor responsiveness of endothelial cells by anatomic context. Am J Pathol 172, 1088–1099 [PubMed: 18292233]
47. Naserian S, Abdelgawad ME, Afshar Bakshloo M, Ha G, Arouche N, Cohen JL, Salomon BL, and Uzan G (2020) The TNF/TNFR2 signaling pathway is a key regulatory factor in endothelial progenitor cell immunosuppressive effect. Cell Commun Signal 18, 94 [PubMed: 32546175]
48. Luo D, Luo Y, He Y, Zhang H, Zhang R, Li X, Dobrucki WL, Sinusas AJ, Sessa WC, and Min W (2006) Differential functions of tumor necrosis factor receptor 1 and 2 signaling in ischemia-mediated arteriogenesis and angiogenesis. Am J Pathol 169, 1886–1898 [PubMed: 17071609]
49. Xing XQ, Li B, Xu SL, Liu J, Zhang CF, and Yang J (2019) MicroRNA-214–3p Regulates Hypoxia-Mediated Pulmonary Artery Smooth Muscle Cell Proliferation and Migration by Targeting ARHGEF12. Med Sci Monit 25, 5738–5746 [PubMed: 31373336]
50. Mosaddeghzadeh N, and Ahmadian MR (2021) The RHO Family GTPases: Mechanisms of Regulation and Signaling. Cells 10
51. Karagkouni D, Paraskevopoulou MD, Chatzopoulos S, Vlachos IS, Tastsoglou S, Kanellos I, Papadimitriou D, Kavakiotis I, Maniou S, Skoufos G, Vergoulis T, Dalamagas T, and Hatzigeorgiou AG (2018) DIANA-TarBase v8: a decade-long collection of experimentally supported miRNA-gene interactions. Nucleic Acids Res 46, D239–D245 [PubMed: 29156006]
52. Baumer Y, Spindler V, Werthmann RC, Bunemann M, and Waschke J (2009) Role of Rac 1 and cAMP in endothelial barrier stabilization and thrombin-induced barrier breakdown. J Cell Physiol 220, 716–726 [PubMed: 19472214]
53. Krendel M, Zenke FT, and Bokoch GM (2002) Nucleotide exchange factor GEF-H1 mediates cross-talk between microtubules and the actin cytoskeleton. Nat Cell Biol 4, 294–301 [PubMed: 11912491]
54. Abe K, Rossman KL, Liu B, Ritola KD, Chiang D, Campbell SL, Burridge K, and Der CJ (2000) Vav2 is an activator of Cdc42, Rac1, and RhoA. J Biol Chem 275, 10141–10149 [PubMed: 10744696]
55. Otani T, Ichii T, Aono S, and Takeichi M (2006) Cdc42 GEF Tuba regulates the junctional configuration of simple epithelial cells. J Cell Biol 175, 135–146 [PubMed: 17015620]
56. Itoh RE, Kurokawa K, Ohba Y, Yoshizaki H, Mochizuki N, and Matsuda M (2002) Activation of rac and cdc42 video imaged by fluorescent resonance energy transfer-based single-molecule probes in the membrane of living cells. Mol Cell Biol 22, 6582–6591 [PubMed: 12192056]
57. Guilluy C, Swaminathan V, Garcia-Mata R, O'Brien ET, Superfine R, and Burridge K (2011) The Rho GEFs LARG and GEF-H1 regulate the mechanical response to force on integrins. Nat Cell Biol 13, 722–727 [PubMed: 21572419]
58. Castillo-Kauil A, Garcia-Jimenez I, Cervantes-Villagrana RD, Adame-Garcia SR, Beltran-Navarro YM, Gutkind JS, Reyes-Cruz G, and Vazquez-Prado J (2020) Galphas directly drives PDZ-RhoGEF signaling to Cdc42. J Biol Chem 295, 16920–16928 [PubMed: 33023908]
59. Thompson WR, Yen SS, Uzer G, Xie Z, Sen B, Styner M, Burridge K, and Rubin J (2018) LARG GEF and ARHGAP18 orchestrate RhoA activity to control mesenchymal stem cell lineage. Bone 107, 172–180 [PubMed: 29208526]
60. Wojciak-Stothard B, Potempa S, Eichholtz T, and Ridley AJ (2001) Rho and Rac but not Cdc42 regulate endothelial cell permeability. J Cell Sci 114, 1343–1355 [PubMed: 11257000]

61. Martin K, Reimann A, Fritz RD, Ryu H, Jeon NL, and Pertz O (2016) Spatio-temporal co-ordination of RhoA, Rac1 and Cdc42 activation during prototypical edge protrusion and retraction dynamics. Sci Rep 6, 21901 [PubMed: 26912264]
62. Michaelson D, Silletti J, Murphy G, D'Eustachio P, Rush M, and Philips MR (2001) Differential localization of Rho GTPases in live cells: regulation by hypervariable regions and RhoGDI binding. J Cell Biol 152, 111–126 [PubMed: 11149925]
63. Solski PA, Helms W, Keely PJ, Su L, and Der CJ (2002) RhoA biological activity is dependent on prenylation but independent of specific isoprenoid modification. Cell Growth Differ 13, 363–373 [PubMed: 12193475]
64. DerMardirossian C, and Bokoch GM (2005) GDIs: central regulatory molecules in Rho GTPase activation. Trends Cell Biol 15, 356–363 [PubMed: 15921909]
65. Ridley AJ (2006) Rho GTPases and actin dynamics in membrane protrusions and vesicle trafficking. Trends Cell Biol 16, 522–529 [PubMed: 16949823]
66. Muller PM, Rademacher J, Bagshaw RD, Wortmann C, Barth C, van Unen J, Alp KM, Giudice G, Eccles RL, Heinrich LE, Pascual-Vargas P, Sanchez-Castro M, Brandenburg L, Mbamalu G, Tucholska M, Spatt L, Czajkowski MT, Welke RW, Zhang S, Nguyen V, Rrustemi T, Trnka P, Freitag K, Larsen B, Popp O, Mertins P, Gingras AC, Roth FP, Colwill K, Bakal C, Pertz O, Pawson T, Petsalaki E, and Rocks O (2020) Systems analysis of RhoGEF and RhoGAP regulatory proteins reveals spatially organized RAC1 signalling from integrin adhesions. Nat Cell Biol 22, 498–511 [PubMed: 32203420]
67. Uechi Y, Bayarjargal M, Umikawa M, Oshiro M, Takei K, Yamashiro Y, Asato T, Endo S, Misaki R, Taguchi T, and Kariya K (2009) Rap2 function requires palmitoylation and recycling endosome localization. Biochem Biophys Res Commun 378, 732–737 [PubMed: 19061864]
68. de Rooij J, Boenink NM, van Triest M, Cool RH, Wittinghofer A, and Bos JL (1999) PDZ-GEF1, a guanine nucleotide exchange factor specific for Rap1 and Rap2. J Biol Chem 274, 38125–38130 [PubMed: 10608883]
69. Kuiperij HB, de Rooij J, Rehmann H, van Triest M, Wittinghofer A, Bos JL, and Zwartkruis FJ (2003) Characterisation of PDZ-GEFs, a family of guanine nucleotide exchange factors specific for Rap1 and Rap2. Biochim Biophys Acta 1593, 141–149 [PubMed: 12581858]
70. Ohba Y, Mochizuki N, Matsuo K, Yamashita S, Nakaya M, Hashimoto Y, Hamaguchi M, Kurata T, Nagashima K, and Matsuda M (2000) Rap2 as a slowly responding molecular switch in the Rap1 signaling cascade. Mol Cell Biol 20, 6074–6083 [PubMed: 10913189]
71. Cherfils J (2014) GEFs and GAPs: Mechanisms and Structures 51–63
72. Rebhun JF, Castro AF, and Quilliam LA (2000) Identification of guanine nucleotide exchange factors (GEFs) for the Rap1 GTPase. Regulation of MR-GEF by M-Ras-GTP interaction. J Biol Chem 275, 34901–34908 [PubMed: 10934204]
73. Kawasaki H, Springett GM, Mochizuki N, Toki S, Nakaya M, Matsuda M, Housman DE, and Graybiel AM (1998) A family of cAMP-binding proteins that directly activate Rap1. Science 282, 2275–2279 [PubMed: 9856955]
74. Crittenden JR, Bergmeier W, Zhang Y, Piffath CL, Liang Y, Wagner DD, Housman DE, and Graybiel AM (2004) CalDAG-GEFI integrates signaling for platelet aggregation and thrombus formation. Nat Med 10, 982–986 [PubMed: 15334074]
75. Pannekoek WJ, Kooistra MR, Zwartkruis FJ, and Bos JL (2009) Cell-cell junction formation: the role of Rap1 and Rap1 guanine nucleotide exchange factors. Biochim Biophys Acta 1788, 790–796 [PubMed: 19159611]
76. Bagci H, Sriskandarajah N, Robert A, Boulais J, Elkholi IE, Tran V, Lin ZY, Thibault MP, Dube N, Faubert D, Hipfner DR, Gingras AC, and Cote JF (2020) Mapping the proximity interaction network of the Rho-family GTPases reveals signalling pathways and regulatory mechanisms. Nat Cell Biol 22, 120–134 [PubMed: 31871319]
77. Pannekoek WJ, Vliem MJ, and Bos JL (2020) Multiple Rap1 effectors control Epac1-mediated tightening of endothelial junctions. Small GTPases 11, 346–353 [PubMed: 29388865]
78. Wiggins-Dohlvik K, Merriman M, Shaji CA, Alluri H, Grimsley M, Davis ML, Smith RW, and Tharakan B (2014) Tumor necrosis factor-alpha disruption of brain endothelial cell barrier is

mediated through matrix metalloproteinase-9. Am J Surg 208, 954–960; discussion 960 [PubMed: 25312844]

79. Arthur WT, Quilliam LA, and Cooper JA (2004) Rap1 promotes cell spreading by localizing Rac guanine nucleotide exchange factors. J Cell Biol 167, 111–122 [PubMed: 15479739]
80. Marei H, and Malliri A (2017) GEFs: Dual regulation of Rac1 signaling. Small GTPases 8, 90–99 [PubMed: 27314616]
81. Cullere X, Shaw SK, Andersson L, Hirahashi J, Luscinskas FW, and Mayadas TN (2005) Regulation of vascular endothelial barrier function by Epac, a cAMP-activated exchange factor for Rap GTPase. Blood 105, 1950–1955 [PubMed: 15374886]
82. Sehrawat S, Cullere X, Patel S, Italiano J Jr., and Mayadas TN (2008) Role of Epac1, an exchange factor for Rap GTPases, in endothelial microtubule dynamics and barrier function. Mol Biol Cell 19, 1261–1270 [PubMed: 18172027]
83. Ramos CJ, Lin C, Liu X, and Antonetti DA (2018) The EPAC-Rap1 pathway prevents and reverses cytokine-induced retinal vascular permeability. J Biol Chem 293, 717–730 [PubMed: 29158262]

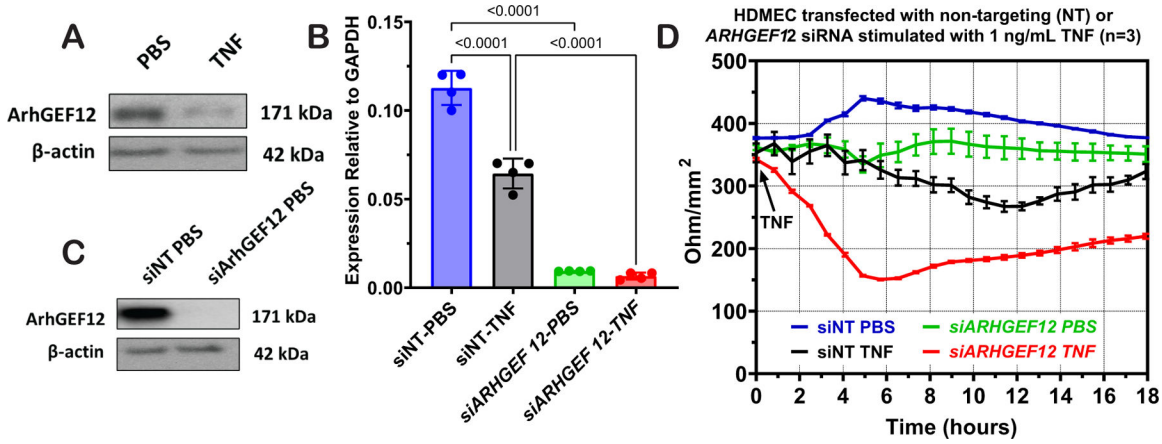

Figure. 1. TNF reduces TEER by disrupting barrier function in ArhGEF12 depleted human dermal microvascular endothelial cell (HDMEC).

A, Human dermal microvascular endothelial cells (HDMECs) treated with TNF (1 ng/mL, 6 hours) shows reduced level of ArhGEF12 compared to those treated with saline (PBS). **B,** HDMECs transfected with non-targeting siRNA (siNT) or *ARHGEF12* targeted siRNA, (si-*ARHGEF12*) demonstrate efficient knockdown of *ARHGEF12* transcript, mRNA levels are expressed as the means relative to the housekeeping gene glyceraldehyde 3-phosphate dehydrogenase (GAPDH) with standard deviation (n=3). Results are expressed as the means relative to control with standard deviation, n=3). **C,** HDMECs transfected with *ARHGEF12* siRNA demonstrate depleted ArhGEF12 protein. **D**, TEER changes in HDMECs transfected with si-NT or si-*ARHGEF12* was recorded between 48–72 hours of transfection stimulated in the presence and absence of TNF (1 ng/mL, 6 hours) without replacing the growth medium at 24-hour post-feeding. The y-axis shows absolute TEER relative to electrode surface area. HDMECs depleted of ArhGEF12 demonstrate earlier and more severe TNF induced leak. Error bars represent standard deviation (n=3). Ordinary one-way analysis of variance (One-way ANOVA) was performed to compare the means of multiple two groups (n=3). Significance indicated by p-value above comparison bars.

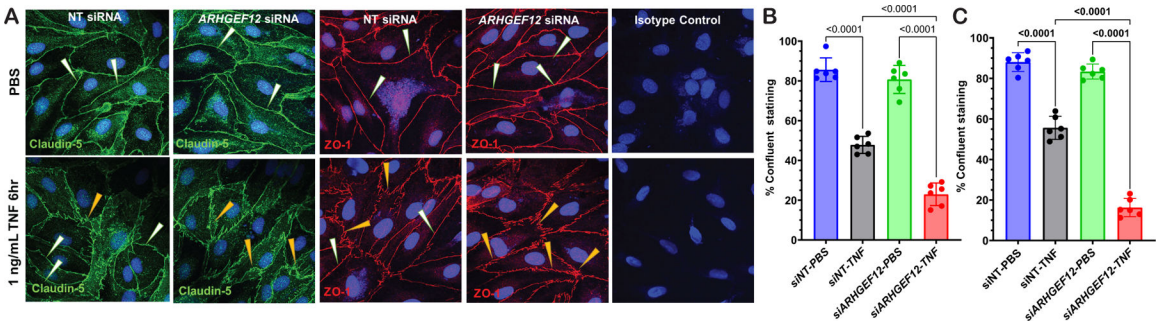

Figure 2. ArhGEF12 knockdown disrupts TNF-induced tight junction disorganization.

A, Confocal immunofluorescence staining was performed to assess the organization of tight junction proteins claudin-5 and ZO-1. Human dermal microvascular endothelial cells (HDMECs) treated with non-targeting siRNA (NT siRNA) or ARHGEF12 siRNA were stimulated with TNF at 1 ng/mL or saline (PBS) for 6 hours were analyzed for claudin-5 (green) ZO-1 (red). Both groups of HDMECs treated with PBS display smooth, confluent circumferential staining of claudin-5 or ZO-1 (A, top row of panels, white arrows). HDMECs treated with NT siRNA and TNF display both disrupted “saw-tooth” staining (A, bottom row of panels, yellow arrows) and smooth staining (A, bottom row of panels, white arrow). However, HDMECs depleted of ArhGEF12 and stimulated with TNF (1 ng/mL, 6 hours) display an increase in the extent of disrupted junctional staining (A, bottom row of panels, yellow arrows). Results are typical of 3 separate experiments (scale bar =25 μm). Quantification of confluent smooth staining of claudin-5 (**B**) and ZO-1 (**C**) reveal dramatically disrupted staining in the *ARHGEF12* siRNA transfected cells with preserved junctional staining in the NT siRNA transfected cells. Ordinary one-way analysis of variance (One-way ANOVA) was performed to compare the means of multiple groups (n=3). Significance indicated by p-value above comparison bars.

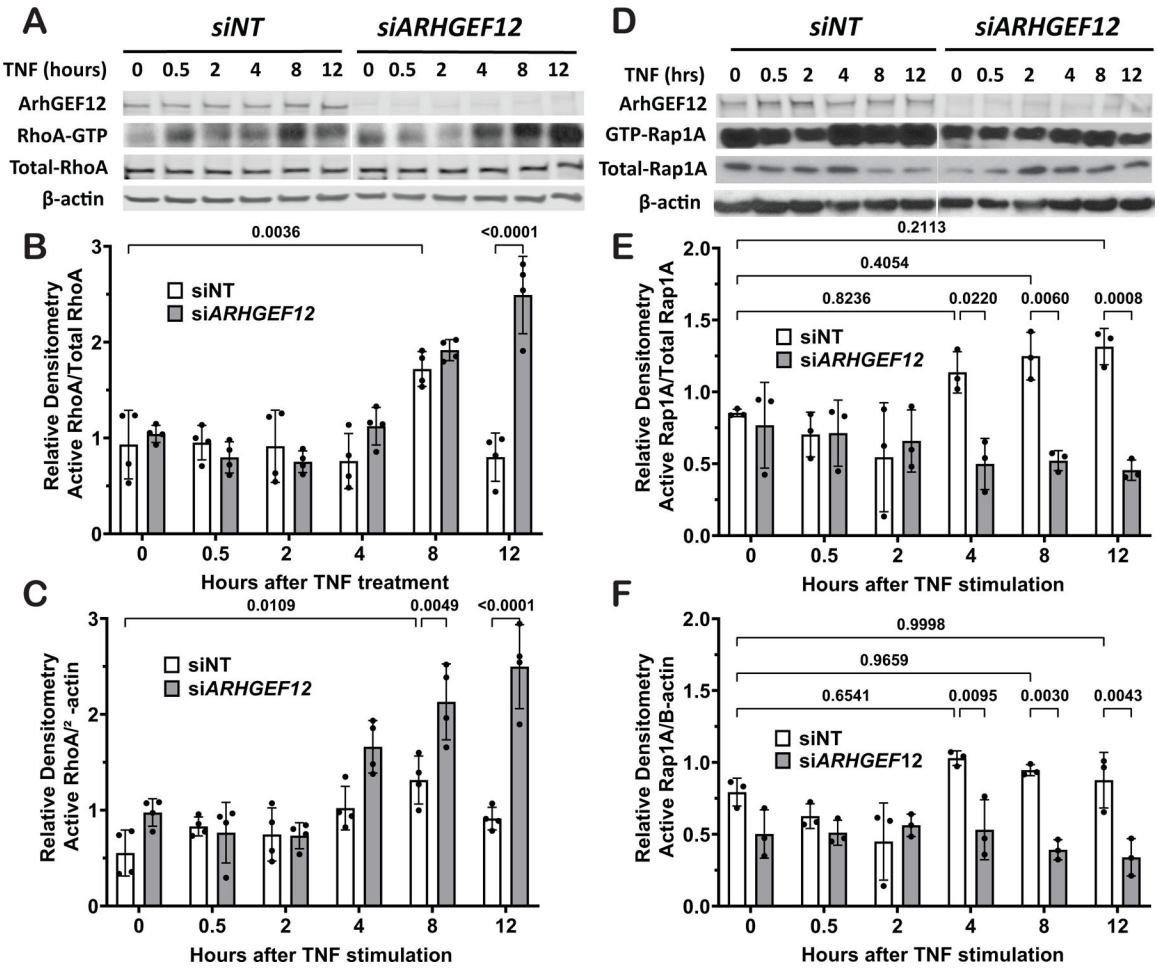

Figure 3: ArhGEF12 depletion reduces the amount of active Rap1A and increases the amount of active RhoA.

A–B, Human dermal microvascular endothelial cells (HDMECs) transfected with ARHGEF12 siRNA (siARHGEF12) and stimulated with TNF (1 ng/mL, 0 – 12 hours) demonstrate significant reduction in the levels of active Rap1A but RhoA relative to the loading control β-actin and total Rap1A (containing both inactive GDP-bound and active GTP-bound forms). In HDMECs depleted of ArhGEF12, there is significant reduction in the total and active Rap1A (quantification E & F) but no reduction in the total and active RhoA (quantification B–C). Results are expressed as the means relative to non-targeting PBS group with standard deviation, n=3. Two-way analysis of variance (Two-way ANOVA) was performed to compare multiple groups (n=3). Significance indicated by p-value above comparison bars.

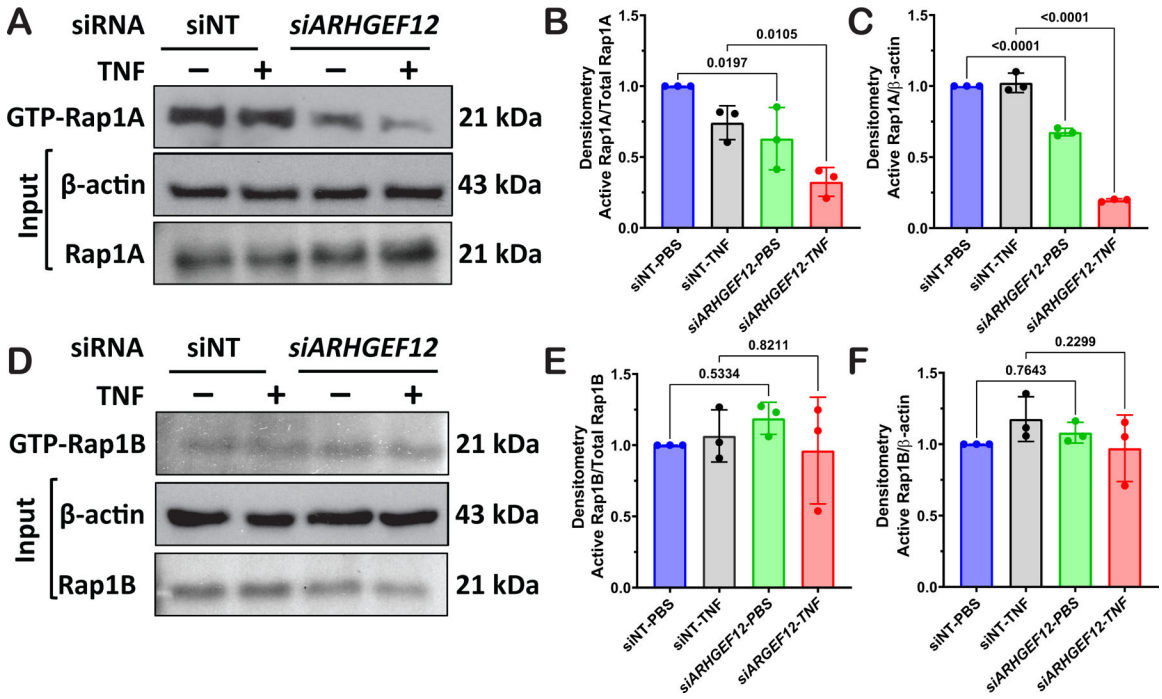

Figure 4. ArhGEF12 depletion reduces the total amount of active GTP-bound RAP1A.

A – B. Human dermal microvascular endothelial cells (HDMECs) transfected with *ARHGEF12* siRNA (si*ARHGEF12*) and stimulated with TNF (1 ng/mL, 6 hours) demonstrate decreased levels of active Rap1A relative to the loading control β-actin and total Rap1A (containing both inactive GDP-bound and active GTP-bound forms) versus other Rap1B isoform. In HDMECs depleted of ArhGEF12, there is significant decrease in the active Rap1A (A, quantification, C & E), but no change in total and active Rap1B isoform (B, quantification D & F). Results are expressed as the means relative to non-targeting PBS group with standard deviation, n=3. The density of the proteins in each control (NT-PBS) group was used as a standard (1 arbitrary unit) to compare the relative density of the other groups. Ordinary one-way analysis of variance (One-way ANOVA) was performed to compare the means of multiple groups (n=3). Significance indicated by p-value above comparison bars.

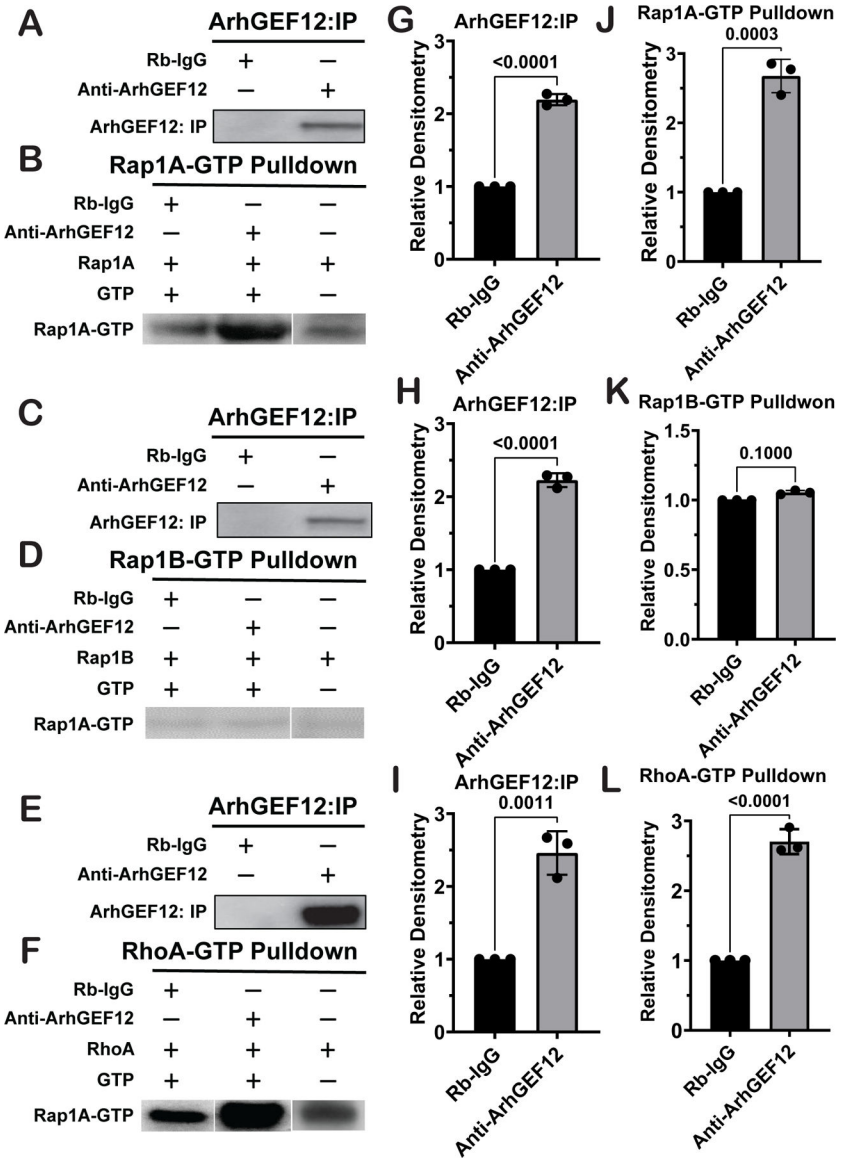

Figure 5. ArhGEF12 is a specific GTP exchange factor for Rap1A and RhoA and not Rap1B.

ArhGEF12 was immuno-precipitated prior to each cell free assay (Fig 5 A, C, E quantification relative to IgG pulldown G, H, I, n=3). Immunoprecipitated ArhGEF12 in the presence and absence of GTP was incubated with recombinant Rap1A, Rap1B and RhoA proteins, and assessed by pulldown assay. Pulldown of active Rap1A, Rap1B and RhoA after incubation demonstrate a dramatic increase in GTP loaded Rap1A (B, quantification relative to GTP loading in the IgG group, J) and RhoA (F, quantification relative to GTP loading in IgG group, L) but no change in GTP loaded Rap1B (D, quantification relative to GTP loading in IgG group, K). Results are expressed as the means of three different experiments. The density of the proteins in each control (Rb-IgG) group was used as a standard (1 arbitrary unit) to compare the relative density of the other groups. Paired t- tests were used to compare groups (n=3). Significance indicated by p-value above comparison bars.

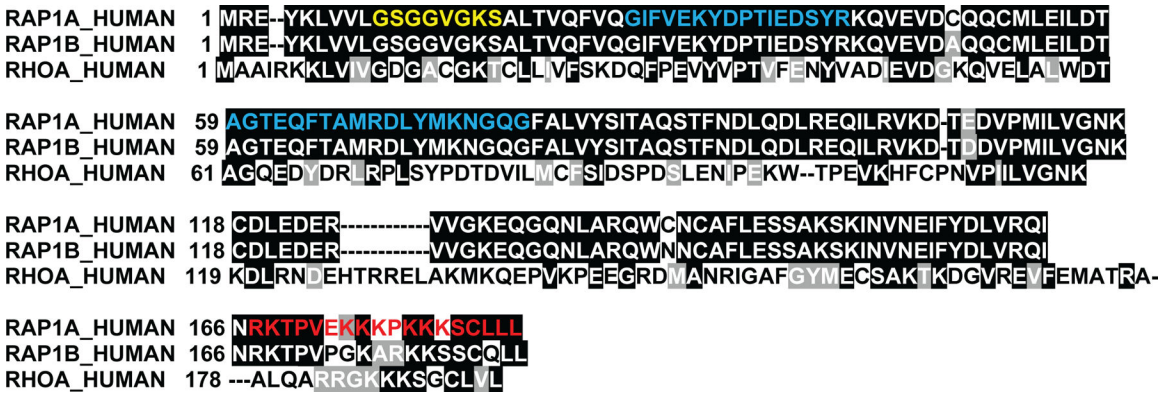

Figure 6: Sequence alignment of Rap1A, Rap1B and RhoA.

Rap1A and Rap1B share 95% sequence identity. RhoA shares 30% sequence identity with Rap1A. The P-loop, in yellow text, is important for nucleotide binding. The first and second switch regions, in blue text, are important for GEF and effector protein binding. Notably, these regions are 100% identical between Rap1A and Rap1B. The hypervariable regions, shown in red text, is important for fatty acid modification that is important for sub-cellular localization.

Table 1.

Analysis of *ARHGEF12* expression in human dermal microvascular endothelial cells (HDMECs) and human umbilical vein endothelial cells (HUVECs). Under identical culture conditions, ECs were treated with 0.5 ng/mL TNF for 6 hours before whole transcriptome analysis. *ARHGEF12* is significantly greater expressed in HDMECs before TNF stimulation (row 1) and is significantly downregulated in HDMECs after TNF treatment (row 2) but not in HUVECs (row 3) suggesting its importance in the regulation of tight junctions, formed in HDMECs but not HUVECs. Datasets are deposited in Gene Expression Omnibus for HDMEC; GSE161021, and HUVEC; GSE190181.

Gene	Condition 1	Condition 2	Log_2 Fold Change	q Value	Significant
ARHGEF12	HDMEC PBS	HUVEC PBS	−0.857488	0.000163	Yes
ARHGEF12	HDMEC PBS	HDMEC TNF	−0.462161	0.000163	Yes
ARHGEF12	HUVEC PBS	HUVEC TNF	−0.0621693	0.678816	No